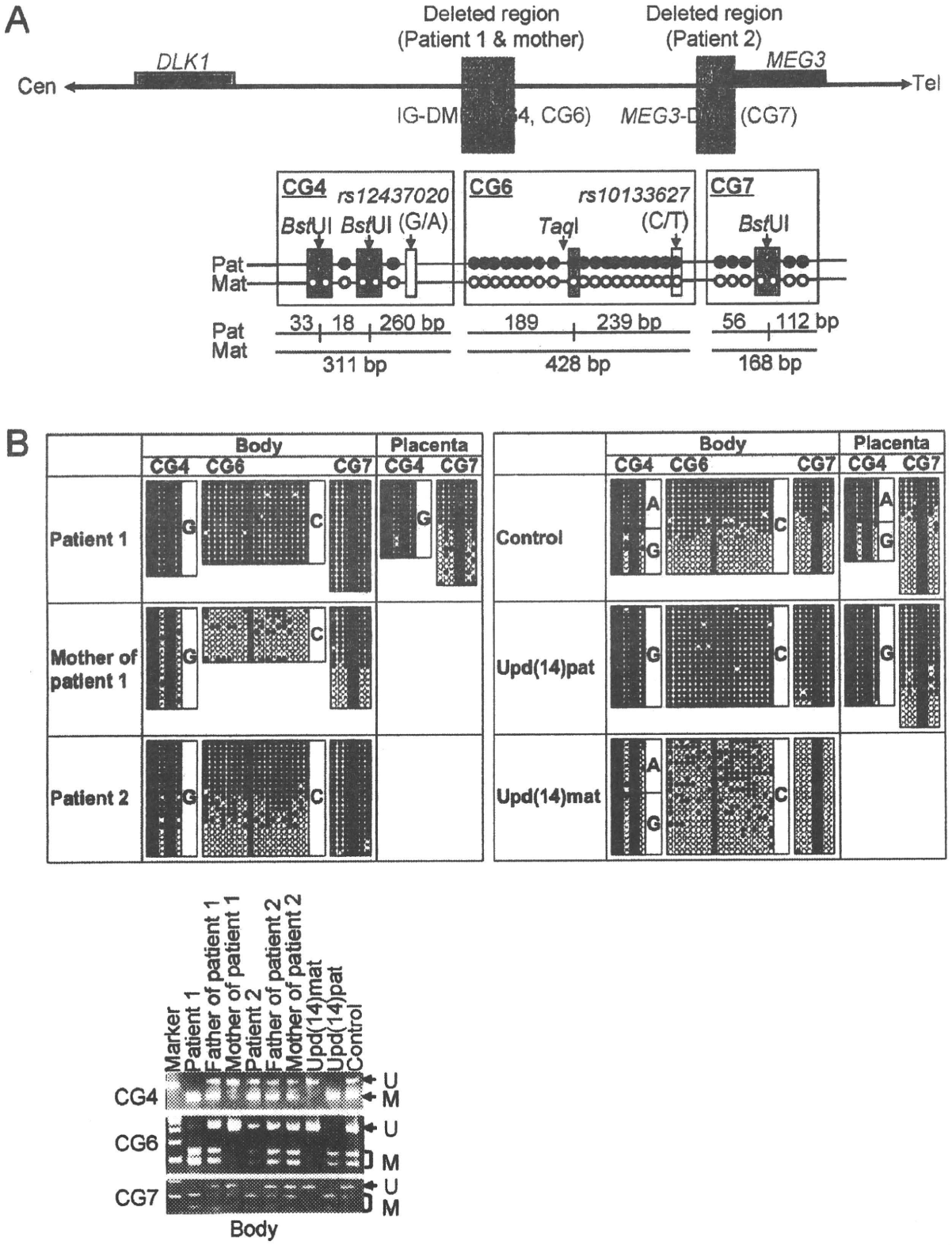

Figure 3. Methylation analysis of the IG-DMR (CG4 and CG6) and the *MEG3*-DMR (CG7). Filled and open circles indicate methylated and unmethylated cytosines at the CpG dinucleotides, respectively. (A) Structure of CG4, CG6, and CG7. Pat: paternally derived chromosome; and Mat:

maternally derived chromosome. The PCR products for CG4 (311 bp) harbor 6 CpG dinucleotides and a G/A SNP (*rs12437020*), and are digested with *Bst*UI into three fragment (33 bp, 18 bp, and 260 bp) when the cytosines at the first and the second CpG dinucleotides and the fourth and the fifth CpG dinucleotides (indicated with orange rectangles) are methylated. The PCR products for CG6 (428 bp) carry 19 CpG dinucleotides and a C/T SNP (*rs10133627*), and are digested with *Taq*I into two fragment (189 bp and 239 bp) when the cytosine at the 9th CpG dinucleotide (indicated with an orange rectangle) is methylated. The PCR products for CG7 harbor 7 CpG dinucleotides, and are digested with *Bst*UI into two fragment (56 bp and 112 bp) when the cytosines at the fourth and the fifth CpG dinucleotides (indicated with orange rectangles) are methylated. These enzymes have been utilized for combined bisulfite restriction analysis (COBRA). (B) Methylation analysis. Upper part shows bisulfite sequencing data. The SNP typing data are also denoted for CG4 and CG6. The circles highlighted in orange correspond to those shown in Figure 3A. The relatively long CG6 was not amplified from the formalin-fixed and paraffin-embedded placental samples, probably because of the degradation of genomic DNA. Note that CG4 is differentially methylated in a control placenta and is massively hypermethylated in a upd(14)pat placenta, whereas CG7 is rather hypomethylated in a upd(14)pat placenta as well as in a control placenta. Lower part shows COBRA data. U: unmethylated clone specific bands (311 bp for CG4, 428 bp for CG6, and 168 bp for CG7); and M: methylated clone specific bands (260 bp for CG4, 239 bp and 189 bp for CG6, and 112 bp and 56 bp for CG7). The results reproduce the bisulfite sequencing data, and delineate normal findings of the father of patient 1 and the parents of patient 2.
doi:10.1371/journal.pgen.1000992.g003

size was 8,558 bp (82,270,449–82,279,006 bp) for the microdeletion in patient 1 and her mother, and 4,303 bp (82,290,978–82,295,280 bp) for the microdeletion in patient 2. The microdeletion in patient 2 also involved the 5′ part of *MEG3* and five of the seven putative CTCF binding sites A–G [10], and was accompanied by insertion of a 66 bp sequence duplicated from *MEG3* intron 5 (82,299,727–82,299,792 bp on NT_026437). Direct sequencing of the exonic or transcribed regions detected no mutation in *DLK1*, *MEG3*, and *RTL1*, although several cDNA polymorphisms (cSNPs) were identified (Table S1). Oligoarray comparative genomic hybridization identified no other discernible structural abnormality (Figure S1B).

Methylation analysis of the two DMRs and the seven putative CTCF binding sites

We next studied methylation patterns of the previously reported IG-DMR (CG4 and CG6) and *MEG3*-DMR (CG7) (Figure 3A) [2], using bisulfite treated gDNA samples. Bisulfite sequencing and combined bisulfite restriction analysis using body samples revealed a hypermethylated IG-DMR and *MEG3*-DMR in patient 1, a hypomethylated IG-DMR and differentially methylated *MEG3*-DMR in the mother of patient 1, and a differentially methylated IG-DMR and hypermethylated *MEG3*-DMR in patient 2, and bisulfite sequencing using placental samples showed a hypermethylated IG-DMR and rather hypomethylated *MEG3*-DMR in patient 1 (Figure 3B).

We also examined methylation patterns of the seven putative CTCF binding sites by bisulfite sequencing (Figure 4A). The sites C and D alone exhibited DMRs in the body and were rather hypomethylated in the placenta (Figure 4B), as observed in CG7. Furthermore, to identify an informative SNP(s) pattern for allele-specific bisulfite sequencing, we examined a 349 bp region encompassing the site C and a 356 bp region encompassing the site D as well as a 300 bp region spanning the previously reported three SNPs near the site D, in 120 control subjects, the cases with upd(14)pat/mat, and patients 1 and 2 and their parents. Consequently, an informative polymorphism was identified for a novel G/A SNP near the site D in only a single control subject, and the parent-of-origin specific methylation pattern was confirmed (Figure 4C). No informative SNP was found in the examined region around the site C, and no other informative SNP was identified in the two examined regions around the site D, with the previously known three SNPs being present in a homozygous condition in all the subjects analyzed.

Expression analysis of the imprinted genes

Finally, we performed expression analyses, using standard reverse transcriptase (RT)-PCR and/or q-PCR analysis for multiple imprinted genes in this region (Figure 5A–5C). For leukocytes, weak expression was detected for *MEG3* and *SNORD114-29* in a control subject and the mother of patient 1 but not in patient 1. For skin fibroblasts, although all *MEGs* but no *PEGs* were expressed in control subjects, neither *MEGs* nor *PEGs* were expressed in patient 2. For placentas, although all imprinted genes were expressed in control subjects, *PEGs* only were expressed in patient 1. For the pituitary and adrenal of patient 2, *DLK1* expression alone was identified.

Expression pattern analyses using informative cSNPs revealed monoallelic *MEG3* expression in the leukocytes of the mother of patient 1 (Figure 5D), and biparental *RTL1* expression in the placenta of patient 1 (no informative cSNP was detected for *DLK1*) and biparental *DLK1* expression in the pituitary and adrenal of patient 2 (*RTL1* was not expressed in the pituitary and adrenal) (Figure 5E), as well as maternal *MEG3* expression in the control leukocytes and paternal *RTL1* expression in the control placentas (Figure S2). Although we also attempted q-PCR analysis, precise assessment was impossible for *MEG3* in the mother of patient 1 because of faint expression level in leukocytes and for *RTL1* in patient 1 and *DLK1* in patient 2 because of poor quality of mRNAs obtained from formalin-fixed and paraffin-embedded tissues.

Discussion

The data of the present study are summarized in Figure 6. Parental origin of the microdeletion positive chromosomes is based on the methylation patterns of the preserved DMRs in patients 1 and 2 and the mother of patient 1 as well as maternal transmission in patient 1. Loss of the hypomethylated IG-DMR of maternal origin in patient 1 was associated with epimutation (hypermethylation) of the *MEG3*-DMR in the body and caused paternalization of the imprinted region and typical upd(14)pat body and placental phenotypes, whereas loss of the hypomethylated *MEG3*-DMR of maternal origin in patient 2 permitted normal methylation pattern of the IG-DMR in the body and resulted in maternal to paternal epigenotypic alteration and typical upd(14)pat body, but no placental, phenotype. In this regard, while a 66 bp segment was inserted in patient 2, this segment contains no known regulatory sequence [11] or evolutionarily conserved element [12] (also examined with a VISTA program, http://genome.lbl.gov/vista/index.shtml). Similarly, while no control samples were available for pituitary and adrenal, the previous study in human subjects has shown paternal *DLK1* expression in adrenal as well as monoallelic *DLK1* and *MEG3* expressions in various tissues [11]. Furthermore, the present and the previous studies [2] indicate that this region is imprinted in the placenta as well as in the body. Thus, these results, in conjunction with the finding that the IG-DMR remains as a DMR and the *MEG3*-DMR exhibits a non-DMR in the placenta [2], imply the following: (1) the IG-DMR functions hierarchically as an upstream regulator for the methylation pattern of the *MEG3*-DMR on the maternally inherited chromosome in the body, but not in the placenta; (2) the hypomethylated

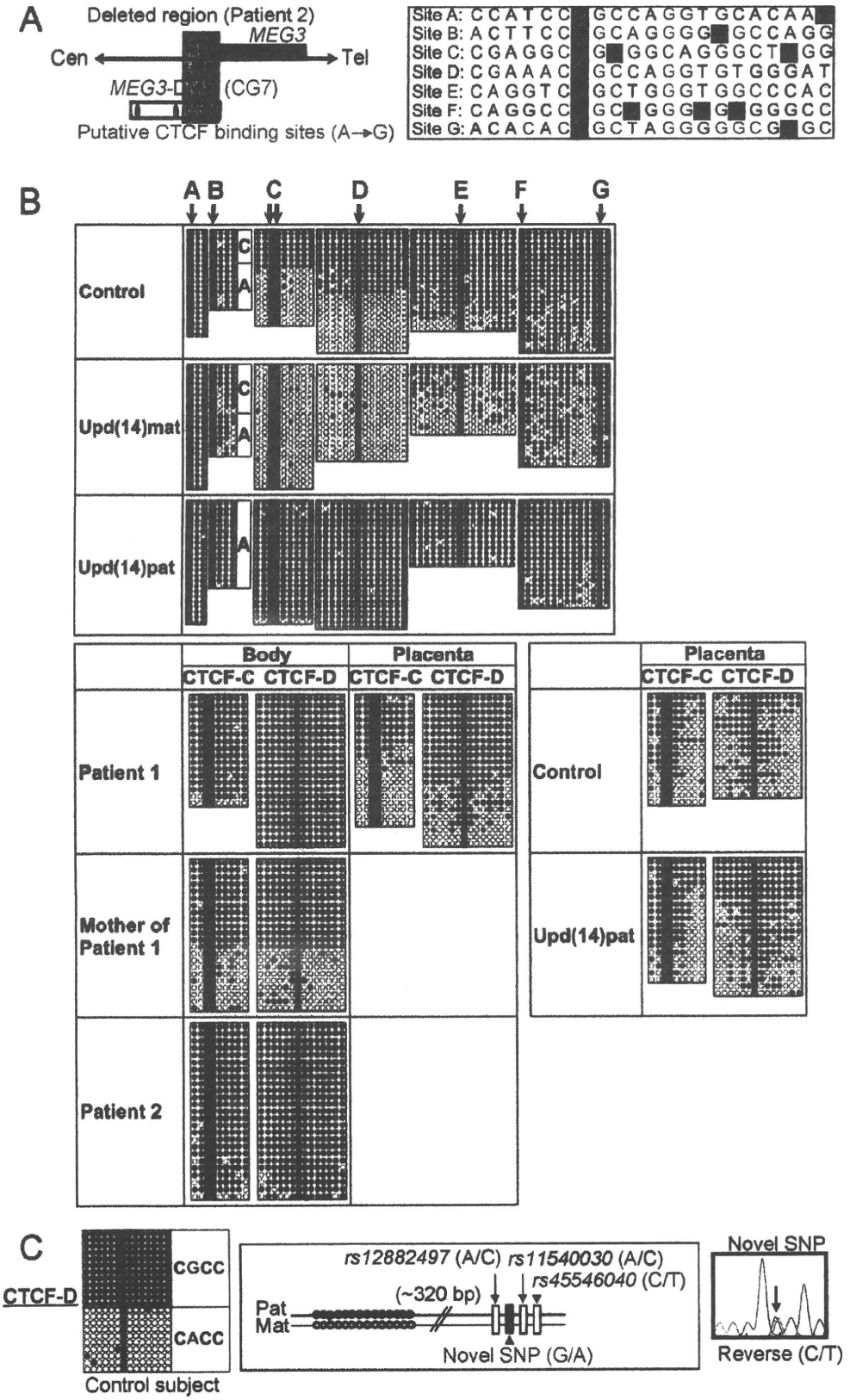
A
Deleted region (Patient 2)
MEG3
Cen
Tel
MEG3-D
(CG7)
Putative CTCF binding sites (A→G)
Site A: C C A T C C G C C A G G T G C A C A A
Site B: A C T T C C G C A G G G G G C C A G G
Site C: C G A G G C G G G C A G G G C T G G
Site D: C G A A A C G C C A G G T G T G G G A T
Site E: C A G G T C G C T G G G T G G C C C A C
Site F: C A G G C C G C G G G G G G G C C
Site G: A C A C A C G C T A G G G G G C G G C
B
A B C D E F G
Control
Upd(14)mat
Upd(14)pat
Body
Placenta
CTCF-C CTCF-D
CTCF-C CTCF-D
Patient 1
Mother of Patient 1
Patient 2
Placenta
CTCF-C CTCF-D
Control
Upd(14)pat
C
CTCF-D
CGCC
CACC
Control subject
rs12882497 (A/C) rs11540030 (A/C)
rs45546040 (C/T)
(~320 bp)
Pat
Mat
Novel SNP (G/A)
Novel SNP
Reverse (C/T)

Figure 4. Methylation analysis of the putative CTCF protein binding sites A–G. (A) Location and sequence of the putative CTCF binding sites. In the left part, the sites C and D are painted in yellow and the remaining sites in purple. In the right part, the consensus CTCF binding motifs are shown in red letters; the cytosine residues at the CpG dinucleotides within the CTCF binding motifs are highlighted in blue, and those outside the CTCF binding motifs are highlighted in green [10]. (B) Methylation analysis. Upper part shows bisulfite sequencing data, using leukocyte genomic DNA samples. Since PCR products for the site B contain a C/A SNP (*rs11627993*), genotyping data are also indicated. The circles highlighted in blue correspond to those shown in Figure 4A. The sites C and D exhibit clear DMRs. Lower part indicates the results of the sites C and D using leukocyte and/or placental genomic DNA samples. The findings are similar to those of CG7. (C) Allele-specific methylation pattern of the CTCF binding site D. A novel G/A SNP has been identified in a single control subject, as shown on a reverse chromatogram delineating a C/T SNP pattern, while the previously reported three SNPs were present in a homozygous condition. Methylated and unmethylated clones are associated with the "G" and the "A" alleles, respectively.
doi:10.1371/journal.pgen.1000992.g004

MEG3-DMR functions as an essential imprinting regulator for both *PEGs* and *MEGs* in the body; and (3) in the placenta, the hypomethylated IG-DMR directly controls the imprinting pattern of both *PEGs* and *MEGs*. These notions also explain the epigenotypic alteration in the previous cases with epimutations or microdeletions affecting both DMRs (Figure S3).

It remains to be clarified how the IG-DMR and the *MEG3*-DMR interact hierarchically in the body. However, the present data, together with the previous findings in cases with epimutations [2,5–8], imply that *MEG3*-DMR can remain hypomethylated only in the presence of a hypomethylated IG-DMR and is methylated when the IG-DMR is deleted or methylated irrespective of the parental origin. Furthermore, mouse studies have suggested that the methylation pattern of the postfertilization-derived *Gtl2*-DMR (the mouse homolog for the *MEG3*-DMR) is dependent on that of the germline-derive IG-DMR [13]. Thus, a preferential binding of some factor(s) to the unmethylated IG-DMR may cause a conformational alteration of the genomic structure, thereby protecting the methylation of the *MEG3*-DMR.

It also remains to be elucidated how the IG-DMR and the *MEG3*-DMR regulate the expression of both *PEGs* and *MEGs* in the placenta and the body, respectively. For the *MEG3*-DMR, however, the CTCF binding sites C and D may play a pivotal role in the imprinting regulation. The methylation analysis indicates that the two sites reside within the *MEG3*-DMR, and it is known that the CTCF protein with versatile functions preferentially binds to unmethylated target sequences including the sites C and D [10,14–16]. In this regard, all the *MEGs* in this imprinted region can be transcribed together in the same orientation and show a strikingly similar tissue expressions pattern [1,12], whereas *PEGs* are transcribed in different directions and are co-expressed with *MEGs* only in limited cell-types [1,17]. It is possible, therefore, that preferential CTCF binding to the grossly unmethylated sites C and D activates all the *MEGs* as a large transcription unit and represses all the *PEGs* perhaps by influencing chromatin structure and histone modification independently of the effects of expressed *MEGs*. In support of this, CTCF protein acts as a transcriptional activator for *Gtl2* (the mouse homolog for *MEG3*) in the mouse [18].

Such an imprinting control model has not been proposed previously. It is different from the CTCF protein-mediated insulator model indicated for the *H19*-DMR and from the non-coding RNA-mediated model implicated for several imprinted regions including the KvDMR1 [19]. However, the KvDMR1 harbors two putative CTCF binding sites that may mediate non-coding RNA independent imprinting regulation [20], and the imprinting control center for Prader-Willi syndrome [21] also carries three CTCF binding sites (examined with a Search for CTCF DNA Binding Sites program, http://www.essex.ac.uk/bs/molonc/spa.html). Thus, while each imprinted region would be regulated by a different mechanism, a CTCF protein may be involved in the imprinting control of multiple regions, in various manners.

This imprinted region has also been studied in the mouse. Clinical and molecular findings in wildtype mice [1,22,23], mice with PatDi(12) (paternal disomy for chromosome 12 harboring this imprinted region) [13,24,25], and mice with targeted deletions for the IG-DMR (ΔIG-DMR) [22,26] and for the *Gtl2*-DMR (Δ*Gtl2*-DMR) [27] are summarized in Table 2. These data, together with human data, provide several informative findings. First, in both the human and the mouse, the IG-DMR is differentially methylated in both the body and the placenta, whereas the *MEG3/Gtl2*-DMR is differentially methylated in the body and exhibits non-DMR in the placenta. Second, the IG-DMR and the *MEG3/Gtl2*-DMR show a hierarchical interaction on the maternally derived chromosome in both the human and the mouse bodies. Indeed, the *MEG3/Gtl2*-DMR is epimutated in patient 1 and mice with maternally inherited ΔIG-DMR, and the IG-DMR is normally methylated in patient 2 and mice with maternally inherited Δ*Gtl2*-DMR. Third, the function of the IG-DMR is comparable between human and mouse bodies and different between human and mouse placentas. Indeed, patient 1 has upd(14)pat body and placental phenotypes, whereas mice with the ΔIG-DMR of maternal origin have PatDi(12)-compatible body phenotype and apparently normal placental phenotype. It is likely that imprinting regulation in the mouse placenta is contributed by some mechanism(s) other than the methylation pattern of the IG-DMR, such as chromatin conformation [22,28,29].

Unfortunately, however, the data of Δ*Gtl2*-DMR mice appears to be drastically complicated by the retained neomycin cassette in the upstream region of *Gtl2*. Indeed, it has been shown that the insertion of a *lacZ* gene or a neomycin gene in the similar upstream region of *Gtl2* causes severely dysregulated expression patterns and abnormal phenotypes after both paternal and maternal transmissions [30,31], and that deletion of the inserted neomycin gene results in apparently normal expression patterns and phenotypes after both paternal and maternal transmissions [31]. (In this regard, although a possible influence of the inserted 66 bp segment can not be excluded formally in patient 2, phenotype and expression data in patient 2 are compatible with simple paternalization of the imprinted region.) In addition, since the apparently normal phenotype in mice homozygous for Δ*Gtl2*-DMR is reminiscent of that in sheep homozygous for the callipyge mutation [32], a complicated mechanism(s) such as the polar overdominance may be operating in the Δ*Gtl2*-DMR mice [33]. Thus, it remains to be clarified whether the *MEG3/Gtl2*-DMR has a similar or different function between the human and the mouse.

Two points should be made in reference to the present study. First, the proposed functions of the two DMRs are based on the results of single patients. This must be kept in mind, because there might be a hidden patient-specific abnormality or event that might explain the results. For example, the abnormal placental phenotype in patient 1 might be caused by some co-incidental aberration, and the apparently normal placenta in patient 2 might be due to mosaicism with grossly preserved *MEG3*-DMR in the placenta and grossly deleted *MEG3*-DMR in the body. Second,

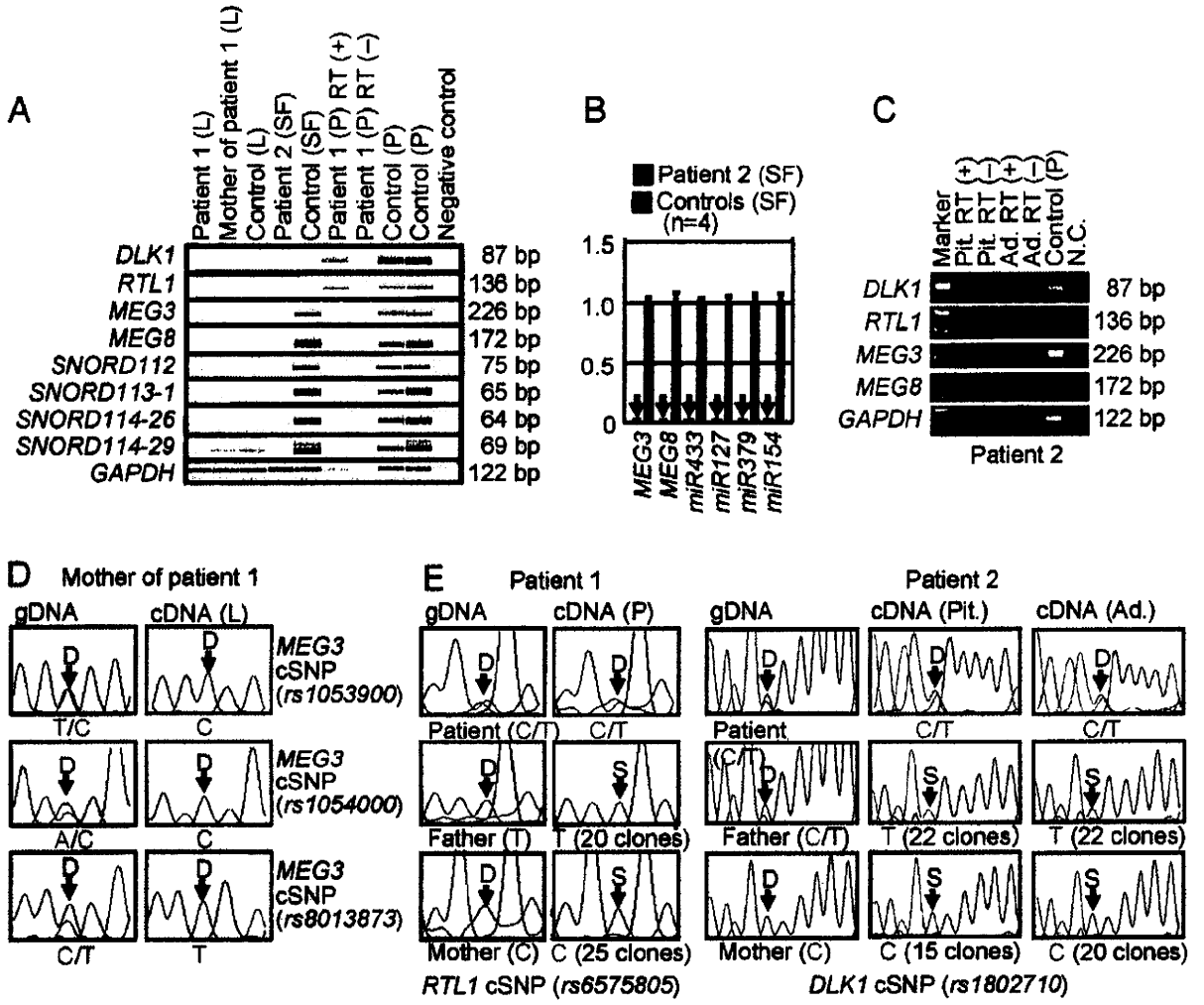

Figure 5. Expression analysis. (A) Reverse transcriptase (RT)-PCR analysis. L: leukocytes; SF: skin fibroblasts; and P: placenta. The relatively weak *GAPDH* expression for the formalin-fixed and paraffin-embedded placenta of patient 1 indicates considerable mRNA degradation. Since a single exon was amplified for *DLK1* and *RTL1*, PCR was performed with and without RT for the placenta of patient 1, to exclude the possibility of false positive results caused by genomic DNA contamination. (B) Quantitative real-time PCR (q-PCR) analysis of *MEG3*, *MEG8*, and *miRNAs*, using fresh skin fibroblasts (SF) of patient 2 and four control neonates. Of the examined *MEGs*, *miR433* and *miR127* are encoded by *RTL1as*. (C) RT-PCR analysis for the formalin-fixed and paraffin-embedded pituitary (Pit.) and the adrenal (Ad.) in patient 2. The bands for *DLK1* are detected in the presence of RT and undetected in the absence of RT, thereby excluding contamination of genomic DNA. (D) Monoallelic *MEG3* expression in the leukocytes of the mother of patient 1. The three cSNPs are present in a heterozygous status in gDNA and in a hemizygous status in cDNA. D: direct sequence. (E) Biparental *RTL1* expression in the placenta of patient 1 and biparental *DLK1* expression in the pituitary and adrenal of patient 2. D: direct sequence; and S: subcloned sequence. In patient 1, genotyping of *RTL1* cSNP (*rs6575805*) using gDNA indicates maternal origin of the "C" allele and paternal origin of the "T" allele, and sequencing analysis using cDNA confirms expression of maternally as well as paternally derived *RTL1*. Similarly, in patient 2, genotyping of *DLK1* cSNP (*rs1802710*) using gDNA denotes maternal origin of the "C" allele and paternal origin of the "T" alleles, and sequencing analysis using cDNA confirms expression of maternally as well as paternally inherited *DLK1*.
doi:10.1371/journal.pgen.1000992.g005

the clinical features in the mother of patient 1 such as short stature and obesity are often observed in cases with upd(14)mat (Table S2). However, the clinical features are non-specific and appear to be irrelevant to the microdeletion involving the IG-DMR, because loss of the paternally derived IG-DMR does not affect the imprinted status [2,26]. Indeed, *MEG3* in the mother of patient 1 showed normal monoallelic expression in the presence of the differentially methylated *MEG3*-DMR. Nevertheless, since the upd(14)mat phenotype is primarily ascribed to loss of functional *DLK1* (Figure S3B) [2,34], it might be possible that the microdeletion involving the IG-DMR has affected a *cis*-acting regulatory element for *DLK1* expression (for details, see Note in the legend for Table S2). Further studies in cases with similar microdeletions will permit clarification of these two points.

In summary, the results show a hierarchical interaction and distinct functional properties of the IG-DMR and the *MEG3*-DMR in imprinting control. Thus, this study provides significant advance in the clarification of mechanisms involved in the imprinting regulation at the 14q32.2 imprinted region and the development of upd(14) phenotype.

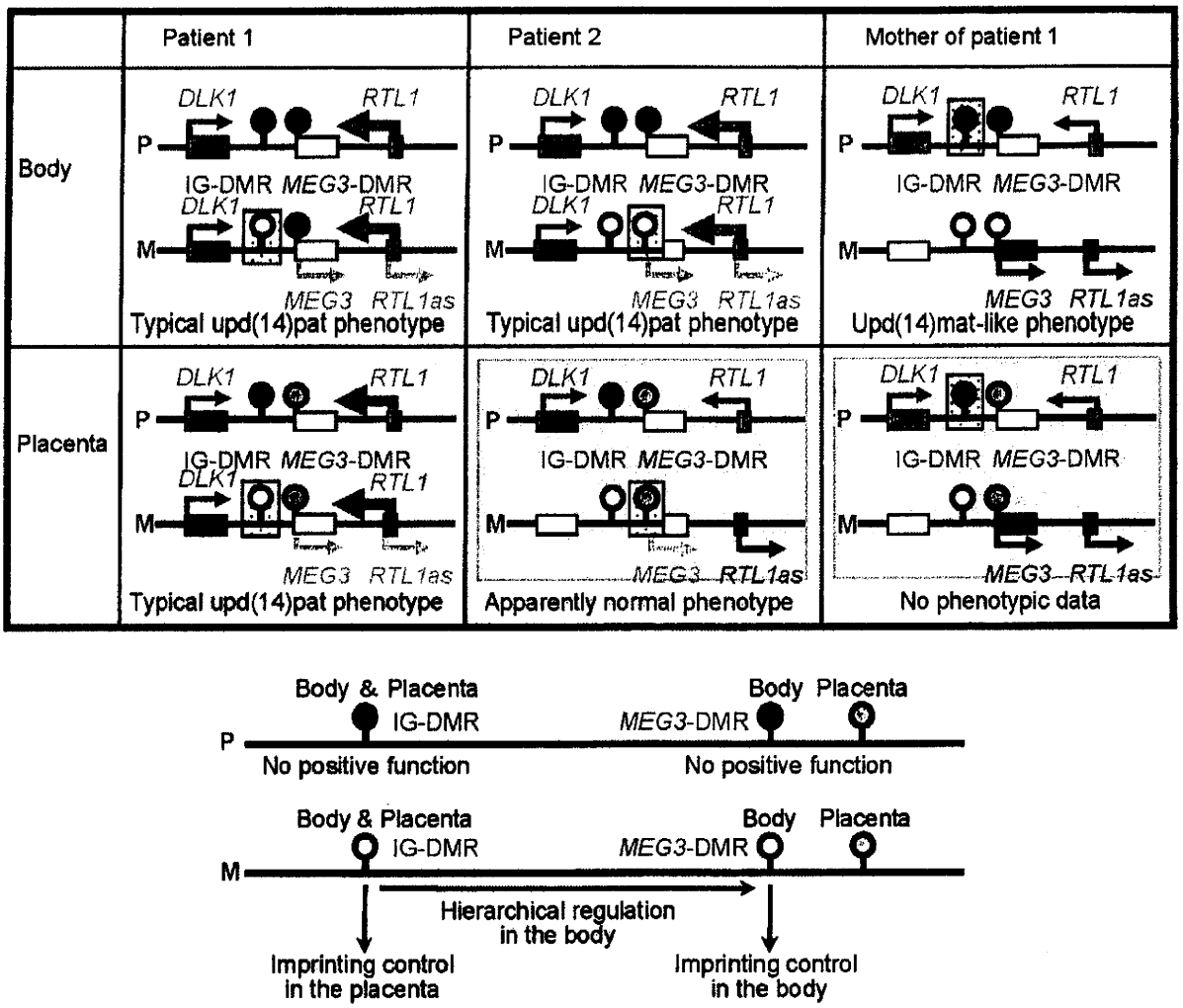

Figure 6. Schematic representation of the observed and predicted methylation and expression patterns. Deleted regions in patients 1 and 2 and the mother of patient 1 are indicated by stippled rectangles. P: paternally derived chromosome; and M: maternally derived chromosome. Representative imprinted genes are shown; these genes are known to be imprinted in the body and the placenta [2] (see also Figure S2). Placental samples have not been obtained in patient 2 and the mother of patient 1 (highlighted with light green backgrounds). Thick arrows for *RTL1* in patients 1 and 2 represent increased *RTL1* expression that is ascribed to loss of functional microRNA-containing *RTL1as* as a repressor for *RTL1* [26,36–38]; this phenomenon has been indicated in placentas with upd(14)pat and in those with an epimutation and a microdeletion involving the two DMRs (Figure S3A and S3C) [2]. *MEG3* and *RTL1as* that are disrupted or predicted to have become silent on the maternally derived chromosome are written in gray. Filled and open circles represent hypermethylated and hypomethylated DMRs, respectively; since the *MEG3*-DMR is rather hypomethylated and regarded as non-DMR in the placenta [2] (see also Figure 3), it is painted in gray.
doi:10.1371/journal.pgen.1000992.g006

Materials and Methods

Ethics statement

This study was approved by the Institutional Review Board Committees at National Center for Child health and Development, University College Dublin, and Dokkyo University School of Medicine, and performed after obtaining written informed consent.

Primers

All the primers utilized in this study are summarized in Table S3.

Sample preparation

For leukocytes and skin fibroblasts, genomic DNA (gDNA) samples were extracted with FlexiGene DNA Kit (Qiagen), and RNA samples were prepared with RNeasy Plus Mini (Qiagen) for *DLK1*, *MEG3*, *RTL1*, *MEG8* and *snoRNAs*, and with mirVana miRNA Isolation Kit (Ambion) for *microRNAs*. For paraffin-embedded tissues including the placenta, brain, lung, heart, liver, spleen, kidney, bladder, and small intestine, gDNA and RNA samples were extracted with RecoverAll Total Nucleic Acids Isolation Kit (Ambion) using slices of 40 μm thick. For fresh control placental samples, gDNA and RNA were extracted using ISOGEN (Nippon Gene). After treating total RNA samples with

Table 2. Clinical and molecular findings in wild-type and PatDi(12) mice and mice with maternally inherited ΔIG-DMR and Δ*Gtl2*-DMR.

	Wildtype	PatDi(12)	ΔIG-DMR (~4.15 kb)[a]	Δ*Gtl2*-DMR (~10 kb)[b]
				Neomycin cassette (+)
<Body>				
Phenotype	Normal	Abnormal[c]	PatDi(12) phenotype[c]	Normal at birth
				Lethal by 4 weeks
Methylation pattern				
IG-DMR	Differential	Methylated	Methylated[d]	Differential
Gtl2-DMR	Differential	Methylated	Epimutated[e]	Methylated[d]
Expression pattern				
Pegs	Monoallelic	Increased (~2x)	Biparental	Grossly normal
			Increased (2x or 4.5x)[f]	
Megs	Monoallelic	Absent	Absent	Decreased (<0.2~0.5x)[g]
<Placenta>				
Phenotype	Normal	Placentomegaly	Apparently normal	Not determined
Methylation pattern				
IG-DMR	Differential	Methylated	Not determined	Not determined
Gtl2-DMR	Non-DMR	Non-DMR	Not determined	Not determined
Expression pattern				
Pegs	Monoallelic	Not determined	Increased (1.5~1.8x)[g]	Decreased (0.5~0.85x)[g]
Megs	Monoallelic	Not determined	Decreased (0.6~0.8x)[g]	Decreased (<0.1~1.0)[g]
Remark			Paternal transmission[h]	Paternal transmission[i]
				Biparental transmission[j]

a The deletion size is smaller than that of patient 1 and her mother in this study, especially at the centromeric region.
b The microdeletion also involves *Gtl2*, and the deletion size is larger than that of patient 2 in this study.
c Body phenotype includes bell-shaped thorax with rib anomalies, distended abdomen, and short and broad neck.
d Hemizygosity for the methylated DMR of paternal origin.
e Hypermethylation of the maternally derived DMR.
f 2x *Dlk1* and *Dio3* expression levels and 4.5x *Rtl1* expression level. The markedly elevated *Rtl1* expression level is ascribed to a synergic effect between activation of the usually silent *Rtl1* of maternal origin and loss of functional microRNA-containing *Rtl1as* as a repressor for *Rtl1* [26,36–38].
g The expression level is variable among examined tissues and examined genes.
h The ΔIG-DMR of paternal origin has permitted normal *Gtl2*-DMR methylation pattern, intact imprinting status, and normal phenotype in the body (no data on the placenta).
i The Δ*Gtl2*-DMR of paternal origin is accompanied by normal methylation pattern of the IG-DMR and variably reduced *Pegs* expression and increased *Megs* expression in the body, and has yielded severe growth retardation accompanied by perinatal lethality.
j The homozygous mutants have survived and developed into fertile adults, despite rather altered expression patterns of the imprinted genes.
doi:10.1371/journal.pgen.1000992.t002

DNase, cDNA samples for *DLK1*, *MEG3*, *MEG8*, and *snoRNAs* were prepared with oligo(dT) primers from 1 μg of RNA using Superscript III Reverse Transcriptase (Invitrogen), and those for *microRNAs* were synthesized from 300 ng of RNA using TaqMan MicroRNA Reverse Transcription Kit (Applied Biosystems). For *RTL1*, cDNA samples were synthesized with *RTL1*-specific primers that do not amplify *RTL1as*. Control gDNA and cDNA samples were extracted from adult leukocytes and neonatal skin fibroblasts purchased from Takara Bio Inc. Japan, and from a fresh placenta of 38 weeks of gestation. Metaphase spreads were prepared from leukocytes and skin fibroblasts using colcemide (Invitrogen).

Structural analysis

Microsatellite analysis and SNP genotyping were performed as described previously [2]. For FISH analysis, metaphase spreads were hybridized with a 5,104 bp FISH-1 probe and a 5,182 bp FISH-2 probe produced by long PCR, together with an RP11-566I2 probe for 14q12 used as an internal control [2]. The FISH-1 and FISH-2 probes were labeled with digoxigenin and detected by rhodamine anti-digoxigenin, and the RP11-566I2 probe was labeled with biotin and detected by avidin conjugated to fluorescein isothiocyanate. For quantitative real-time PCR analysis, the relative copy number to RNaseP (catalog No: 4316831, Applied Biosystems) was determined by the Taqman real-time PCR method using the probe-primer mix on an ABI PRISM 7000 (Applied Biosystems). To determine the breakpoints of microdeletions, sequence analysis was performed for long PCR products harboring the fusion points, using serial forward primers on the CEQ 8000 autosequencer (Beckman Coulter). Direct sequencing was also performed on the CEQ 8000 autosequencer. Oligoarray comparative genomic hybridization was performed with 1×244K Human Genome Array (catalog No: G4411B) (Agilent Technologies), according to the manufacturer's protocol.

Methylation analysis

Methylation analysis was performed for gDNA treated with bisulfite using the EZ DNA Methylation Kit (Zymo Research). After PCR amplification using primer sets that hybridize both methylated and unmethylated clones because of lack of CpG

dinucleotides within the primer sequences, the PCR products were digested with appropriate restriction enzymes for combined bisulfite restriction analysis. For bisulfite sequencing, the PCR products were subcloned with TOPO TA Cloning Kit (Invitrogen) and subjected to direct sequencing on the CEQ 8000 autosequencer.

Expression analysis

Standard RT-PCR was performed for *DLK1*, *RTL1*, *MEG3*, *MEG8*, and *snoRNAs* using primers hybridizing to exonic or transcribed sequences, and one μl of PCR reaction solutions was loaded onto Gel-Dye Mix (Agilent). Taqman real-time PCR was carried out using the probe-primer mixtures (assay No: Hs00292028 for *MEG3* and Hs00419701 for *MEG8*; assay ID: 001028 for *miR433*, 000452 for *miR127*, 000568 for *miR379*, and 000477 for *miR154*) on the ABI PRISM 7000. Data were normalized against *GAPDH* (catalog No: 4326317E) for *MEG3* and *MEG8* and against *RNU48* (assay ID: 0010006) for the remaining *miRs*. The expression studies were performed three times for each sample.

To examine the imprinting status of *MEG3* in the leukocytes of the mother of patient 1, direct sequence data for informative cSNPs were compared between gDNA and cDNA. To analyze the imprinting status of *RTL1* in the placental sample of patient 1 and that of *DLK1* in the pituitary and adrenal samples of patient 2, RT-PCR products containing exonic cSNPs informative for the parental origin were subcloned with TOPO TA Cloning Kit, and multiple clones were subjected to direct sequencing on the CEQ 8000 autosequencer. Furthermore, *MEG3* expression pattern was examined using leukocyte gDNA and cDNA samples from multiple normal subjects and leukocyte gDNA samples from their mothers, and *RTL1* expression pattern was analyzed using gDNA and cDNA samples from multiple fresh normal placentas and leukocyte gDNA from the mothers.

Supporting Information

Figure S1 Structural analysis. (A) Quantitative real-time PCR analysis (q-PCR) for four regions (q-PCR-1-4) in patient 2. The q-PCR-1 and q-PCR-2 regions are present in two copies whereas q-PCR-3 and q-PCR-4 regions are present in a single copy in patient 2. The four regions are present in two copies in the parents and a control subject, in a single copy in the two previously reported patients with microdeletions involving the examined regions (Deletion-1 and Deletion-2 are case 2 and case 3 in Kagami et al. [2], respectively), and in three copies in a hitherto unreported case with 46,XX,der(17)t(14;17)(q32.2;p13)pat who have three copies of the 14q32.2 imprinted region. Since the microsatellite locus *D14S985* is present in two copies (Table S1) and the *MEG3*-DMR is deleted (Figure 2) in patient 2, this has served to localize the breakpoints. (B) Oligoarray comparative genomic hybridization for a ~1 Mb imprinted region. All the signals remain within the normal range (-1 SD ~ +1 SD) (shaded in light blue) in patients 1 and 2.
Found at: doi:10.1371/journal.pgen.1000992.s001 (1.17 MB TIF)

Figure S2 Expression analysis. (A) Maternal *MEG3* expression in the leukocytes of normal subjects. Genotyping has been performed for three cSNPs using genomic DNA (gDNA) and cDNA of leukocytes from control subjects and gDNA samples of their mothers, indicating that both maternally and non-maternally (paternally) derived alleles are delineated in the gDNA, whereas maternally inherited alleles alone are identified in cDNA. These three cSNPs have also been studied in the mother of patient 1 (Figure 5D). (B) Paternal *RTL1* expression in the placenta of a normal subject. Genotyping has been carried out for *RTL1* cSNP using gDNA and cDNA samples of a fresh placenta and gDNA sample from the mother, showing that both maternally and non-maternally (paternally) derived alleles are delineated in the gDNA, whereas a non-maternally (paternally) inherited allele alone is detected in cDNA. This cSNP has also been examined in the placenta of patient 1 (Figure 5E). Furthermore, the results confirm that the primers utilized in this study have amplified *RTL1*, but not *RTL1as*.
Found at: doi:10.1371/journal.pgen.1000992.s002 (0.39 MB TIF)

Figure S3 Schematic representation of the observed and predicted methylation and expression patterns in previously reported cases with upd(14)pat/mat-like phenotypes and in normal and upd(14)pat/mat subjects. For the explanations of the illustrations, see the legend for Figure 6. Previous studies have indicated that (1) Epimutation-1, Deletion-1, Deletion-2, and Deletion-3 lead to maternal to paternal epigenotypic alteration; (2) Epimutation-2 results in paternal to maternal epigenotypic alteration; and (3) Deletion-4 and Deletion-5 have no effect on the epigenotypic status [2,5–8,26]. (A) Cases with typical or mild upd(14)pat phenotype. Epimutation-1: Hypermethylation of the IG-DMR and the *MEG3*-DMR of maternal origin in the body, and that of the IG-DMR of maternal origin in the placenta (the *MEG3*-DMR is rather hypomethylated in the placenta) (cases 6–8 in Kagami et al. [2]). Deletion-1: Microdeletion involving *DLK1*, the two DMRs, and *MEG3* on the maternally inherited chromosome (case 2 in Kagami et al. [2]). Deletion-2: Microdeletion involving *DLK1*, the two DMRs, *MEG3*, *RTL1*, and *RTL1as* on the maternally inherited chromosome (cases 3 and 5 in Kagami et al. [2]). Deletion-3: Microdeletion involving the two DMRs, *MEG3*, *RTL1*, and *RTL1as* on the maternally inherited chromosome (case 4 in Kagami et al. [2]). These findings are explained by the following notions: (1) Epimutation (hypermethylation) of the normally hypomethylated IG-DMR of maternal origin directly results in paternalization of the imprinted region in the placenta and indirectly leads to paternalization of the imprinted region in the body via epimutation (hypermethylation) of the usually hypomethylated *MEG3*-DMR of maternal origin. Thus, the epimutation (hypermethylation) is predicted to have impaired the IG-DMR as the primary target, followed by the epimutation (hypermethylation) of the *MEG3*-DMR after fertilization; (2) Loss of the hypomethylated *MEG3*-DMR of maternal origin leads to paternalization of the imprinted region in the body; and (3) Loss of the hypomethylated IG-DMR of maternal origin results in paternalization of the imprinted region in the placenta. Furthermore, epigenotype-phenotype correlations imply that the severity of upd(14)pat phenotype is primarily determined by the *RTL1* expression dosage rather than the *DLK1* expression dosage [2]. (B) Cases with upd(14)mat-like phenotype. Epimutation-2: Hypomethylation of the IG-DMR and the *MEG3*-DMR of paternal origin (Temple et al. [5], Buiting et al. [6], Hosoki et al. [7], and Zechner et al. [8]). Deletion-4: Microdeletion involving *DLK1*, the two DMRs, and *MEG3* on the paternally inherited chromosome (cases 9 and 10 in Kagami et al. [2]). Deletion-5: Microdeletion involving *DLK1*, the two DMRs, *MEG3*, *RTL1*, and *RTL1as* on the paternally inherited chromosome (case 11 in Kagami et al. [2] and patient 3 in Buiting et al. [6]). These findings are consistent with the following notions: (1) Epimutation (hypomethylation) of the normally hypermethylated IG-DMR of paternal origin directly results in maternalization of the imprinted region in the placenta and indirectly leads to maternalization of the imprinted region in the body through epimutation (hypomethylation) of the usually hypermethylated *MEG3*-DMR of paternal origin. Thus, epimutation (hypomethylation) is predicted to have affected the IG-DMR

as the primary target, followed by the epimutation (hypomethylation) of the *MEG3*-DMR after fertilization; and (2) Loss of the hypermethylated DMRs of paternal origin has no effect on the imprinting status [2,26], so that upd(14)mat-like phenotype is primarily ascribed to the additive effects of loss of functional *DLK1* and *RTL1* from the paternally derived chromosome (the effects of loss of *DIO3* appears to be minor, if any [2,35]). Although the *MEGs* expression dosage is predicted to be normal in Deletion-4 and Deletion-5 and doubled in Epimutation-2 as well as in upd(14)mat, it remains to be determined whether the difference in the *MEGs* expression dosage has major clinical effects or not. (C) Normal and upd(14)pat/mat subjects.
Found at: doi:10.1371/journal.pgen.1000992.s003 (2.72 MB TIF)

Table S1 The results of microsatellite and SNP analyses.
Found at: doi:10.1371/journal.pgen.1000992.s004 (0.19 MB DOC)

Table S2 Clinical features in the mother of patient 1.
Found at: doi:10.1371/journal.pgen.1000992.s005 (0.09 MB DOC)

Table S3 Primers utilized in the present study.
Found at: doi:10.1371/journal.pgen.1000992.s006 (0.14 MB DOC)

Author Contributions

Conceived and designed the experiments: MK ACFS TO. Performed the experiments: MK MF KM FK. Analyzed the data: MK TO. Contributed reagents/materials/analysis tools: MJO AJG YW OA NM KM TO. Wrote the paper: TO.

References

1. da Rocha ST, Edwards CA, Ito M, Ogata T, Ferguson-Smith AC (2008) Genomic imprinting at the mammalian Dlk1-Dio3 domain. Trends Genet 24: 306–316.
2. Kagami M, Sekita Y, Nishimura G, Irie M, Kato F, et al. (2008) Deletions and epimutations affecting the human 14q32.2 imprinted region in individuals with paternal and maternal upd(14)-like phenotypes. Nat Genet 40: 237–242.
3. Kagami M, Yamazawa K, Matsubara K, Matsuo N, Ogata T (2008) Placentomegaly in paternal uniparental disomy for human chromosome 14. Placenta 29: 760–761.
4. Kotzot D (2004) Maternal uniparental disomy 14 dissection of the phenotype with respect to rare autosomal recessively inherited traits, trisomy mosaicism, and genomic imprinting. Ann Genet 47: 251–260.
5. Temple IK, Shrubb V, Lever M, Bullman H, Mackay DJ (2007) Isolated imprinting mutation of the DLK1/GTL2 locus associated with a clinical presentation of maternal uniparental disomy of chromosome 14. J Med Genet 44: 637–640.
6. Buiting K, Kanber D, Martín-Subero JI, Lieb W, Terhal P, et al. (2008) Clinical features of maternal uniparental disomy 14 in patients with an epimutation and a deletion of the imprinted DLK1/GTL2 gene cluster. Hum Mutat 29: 1141–1146.
7. Hosoki K, Ogata T, Kagami M, Tanaka T, Saitoh S (2008) Epimutation (hypomethylation) affecting the chromosome 14q32.2 imprinted region in a girl with upd(14)mat-like phenotype. Eur J Hum Genet 16: 1019–1023.
8. Zechner U, Kohlschmidt N, Rittner G, Damatova N, Beyer V, et al. (2009) Epimutation at human chromosome 14q32.2 in a boy with a upd(14)mat-like clinical phenotype. Clin Genet 75: 251–258.
9. Li E, Beard C, Jaenisch R (1993) Role for DNA methylation in genomic imprinting. Nature 366: 362–365.
10. Rosa AL, Wu YQ, Kwabi-Addo B, Coveler KJ, Reid Sutton V, et al. (2005) Allele-specific methylation of a functional CTCF binding site upstream of MEG3 in the human imprinted domain of 14q32. Chromosome Res 13: 809–818.
11. Wylie AA, Murphy SK, Orton TC, Jirtle RL (2000) Novel imprinted DLK1/GTL2 domain on human chromosome 14 contains motifs that mimic those implicated in IGF2/H19 regulation. Genome Res 10: 1711–1718.
12. Tierling S, Dalbert S, Schoppenhorst S, Tsai CE, Oliger S, et al. (2007) High-resolution map and imprinting analysis of the Gtl2-Dnchc1 domain on mouse chromosome 12. Genomics 87: 225–235.
13. Takada S, Paulsen M, Tevendale M, Tsai CE, Kelsey G, et al. (2002) Epigenetic analysis of the Dlk1-Gtl2 imprinted domain on mouse chromosome 12: implications for imprinting control from comparison with Igf2-H19. Hum Mol Genet 11: 77–86.
14. Ohlsson R, Renkawitz R, Lobanenkov V (2001) CTCF is a uniquely versatile transcription regulator linked to epigenetics and disease. Trends Genet 17: 520–527.
15. Hark AT, Schoenherr CJ, Katz DJ, Ingram RS, Levorse JM, et al. (2000) CTCF mediates methylation-sensitive enhancer-blocking activity at the H19/Igf2 locus. Nature 405: 486–489.
16. Kanduri C, Pant V, Loukinov D, Pugacheva E, Qi CF, et al. (2000) Functional association of CTCF with the insulator upstream of the H19 gene is parent of origin-specific and methylation-sensitive. Curr Biol 10: 853–856.
17. da Rocha ST, Tevendale M, Knowles E, Takada S, Watkins M, et al. (2007) Restricted co-expression of Dlk1 and the reciprocally imprinted non-coding RNA, Gtl2: implications for cis-acting control. Dev Biol 306: 810–823.
18. Wan LB, Pan H, Hannenhalli S, Cheng Y, Ma J, et al. (2008) Maternal depletion of CTCF reveals multiple functions during oocyte and preimplantation embryo development. Development 135: 2729–2738.
19. Ideraabdullah FY, Vigneau S, Bartolomei MS (2008) Genomic imprinting mechanisms in mammals. Mutat Res 647: 77–85.
20. Fitzpatrick GV, Pugacheva EM, Shin JY, Abdullaev Z, Yang Y, et al. (2007) Allele-specific binding of CTCF to the multipartite imprinting control region KvDMR1. Mol Cell Biol 27: 2636–2647.
21. Horsthemke B, Wagstaff J (2008) Mechanisms of imprinting of the Prader-Willi/Angelman region. Am J Med Genet A 146A: 2041–2052.
22. Lin SP, Coan P, da Rocha ST, Seitz H, Cavaille J, et al. (2007) Differential regulation of imprinting in the murine embryo and placenta by the Dlk1-Dio3 imprinting control region. Development 134: 417–426.
23. Coan PM, Burton GJ, Ferguson-Smith AC (2005) Imprinted genes in the placenta–a review. Placenta 26 Suppl A: S10–20.
24. Georgiades P, Watkins M, Surani MA, Ferguson-Smith AC (2000) Parental origin-specific developmental defects in mice with uniparental disomy for chromosome 12. Development 127: 4719–4728.
25. Takada S, Tevendale M, Baker J, Georgiades P, Campbell E, et al. (2000) Delta-like and gtl2 are reciprocally expressed, differentially methylated linked imprinted genes on mouse chromosome 12. Curr Biol 10: 1135–1138.
26. Lin SP, Youngson N, Takada S, Seitz H, Reik W, et al. (2003) Asymmetric regulation of imprinting on the maternal and paternal chromosomes at the Dlk1-Gtl2 imprinted cluster on mouse chromosome 12. Nat Genet 35: 97–102.
27. Takahashi N, Okamoto A, Kobayashi R, Shirai M, Obata Y, et al. (2009) Deletion of Gtl2, imprinted non-coding RNA, with its differentially methylated region induces lethal parent-origin-dependent defects in mice. Hum Mol Genet 18: 1879–1888.
28. Lewis A, Mitsuya K, Umlauf D, Smith P, Dean W, et al. (2004) Imprinting on distal chromosome 7 in the placenta involves repressive histone methylation independent of DNA methylation. Nat Genet 36: 1291–1295.
29. Umlauf D, Goto Y, Cao R, Cerqueira F, Wagschal A, et al. (2004) Imprinting along the Kcnq1 domain on mouse chromosome 7 involves repressive histone methylation and recruitment of Polycomb group complexes. Nat Genet 36: 1296–1300.
30. Sekita Y, Wagatsuma H, Irie M, Kobayashi S, Kohda T, et al. (2006) Aberrant regulation of imprinted gene expression in Gtl2lacZ mice. Cytogenet. Genome Res 113: 223–229.
31. Steshina EY, Carr MS, Glick EA, Yevtodiyenko A, Appelbe OK, et al. (2006) Loss of imprinting at the Dlk1-Gtl2 locus caused by insertional mutagenesis in the Gtl2 5′ region. BMC Genet 7: 44.
32. Charlier C, Segers K, Karim L, Shay T, Gyapay G, et al. (2001) The callipyge mutation enhances the expression of coregulated imprinted genes in cis without affecting their imprinting status. Nat Genet 27: 367–369.
33. Georges M, Charlier C, Cockett N (2003) The callipyge locus: evidence for the trans interaction of reciprocally imprinted genes. Trends Genet 19: 248–252.
34. Moon YS, Smas CM, Lee K, Villena JA, Kim KH, et al. (2002) Mice lacking paternally expressed Pref-1/Dlk1 display growth retardation and accelerated adiposity. Mol Cell Biol 22: 5585–5592.
35. Tsai CE, Lin SP, Ito M, Takagi N, Takada S, et al. (2002) Genomic imprinting contributes to thyroid hormone metabolism in the mouse embryo. Curr Biol 12: 1221–1226.
36. Sekita Y, Wagatsuma H, Nakamura K, Ono R, Kagami M, et al. (2008) Role of retrotransposon-derived imprinted gene, Rtl1, in the feto-maternal interface of mouse placenta. Nat Genet 40: 243–248.
37. Seitz H, Youngson N, Lin SP, Dalbert S, Paulsen M, et al. (2003) Imprinted microRNA genes transcribed antisense to a reciprocally imprinted retrotransposon-like gene. Nat Genet 34: 261–262.
38. Davis E, Caiment F, Tordoir X, Cavaillé J, Ferguson-Smith A, et al. (2005) RNAi-mediated allelic trans-interaction at the imprinted Rtl1/Peg11 locus. Curr Biol 15: 743–749.